Spectroscopic properties and diode end-pumped 2.79 μm laser performance of Er,Pr:GYSGG crystal

Jiakang Chen,[1,2] Dunlu Sun,[1,*] Jianqiao Luo,[1] Huili Zhang,[1,2] Renqin Dou,[1,2] Jingzhong Xiao,[3] Qingli Zhang,[1] and Shaotang Yin[1]

[1] *The Key Laboratory of Photonic Devices and Materials, Anhui Province, Anhui Institute of Optics and Fine Mechanics, Chinese Academy of Sciences, Hefei, 230031, China*
[2] *University of Chinese Academy of Sciences, Beijing, 100049, China*
[3] *CEMDRX, Physics Department, Universidade de Coimbra, Coimbra, P-3004-516, Portugal*
[*] *dlsun@aiofm.ac.cn*

Abstract: We demonstrate a 968 nm diode end-pumped Er,Pr:GYSGG ($Gd_{1.17}Y_{1.83}Sc_2Ga_3O_{12}$) laser at 2.79 μm operated in the pulse and continuous-wave (CW) modes. The lifetimes for the upper laser level $^4I_{11/2}$ and lower level $^4I_{13/2}$ are 0.52 and 0.60 ms, respectively. The laser produces 284 mW of power in the CW mode, corresponding to the optical-to-optical efficiency of 14.8% and slope efficiency of 17.4%. The maximum laser energy achieved is 2.4 mJ at a repetition rate of 50 Hz and pulse duration of 0.5 ms, corresponding to a peak power of 4.8 W and slope efficiency of 18.3%. These results suggest that doping deactivator Pr^{3+} ions can effectively decrease the lower-level lifetime and improve the laser efficiency.

OCIS codes: (140.0140) Lasers and laser optics; (140.3480) Lasers, diode-pumped; (140.3500) Lasers, erbium; (300.6260) Spectroscopy, diode lasers.

References and links

1. M. Tempus, W. Luthy, H. P. Weber, V. G. Ostroumov, and I. A. Shcherbakov, "2.79 μm YSGG:Cr:Er laser pumped at 790 nm," IEEE J. Quantum Electron. **30**(11), 2608–2611 (1994).
2. A. Högele, G. Hörbe, H. Lubatschowski, H. Welling, and W. Ertmer, "2.70 μm CrEr:YSGG laser with high output energy and FTIR-Q-switch," Opt. Commun. **125**(1–3), 90–94 (1996).
3. K. L. Vodopyanov, "Mid-infrared optical parametric generator with extra-wide (3–19-μm) tunability: applications for spectroscopy of two-dimensional electrons in quantum wells," J. Opt. Soc. Am. B **16**(9), 1579–1586 (1999).
4. K. L. Vodopyanov, F. Ganikhanov, J. P. Maffetone, I. Zwieback, and W. Ruderman, "$ZnGeP_2$ optical parametric oscillator with 3.8-12.4- μm tunability," Opt. Lett. **25**(11), 841–843 (2000).
5. V. Lupei, S. Georgescu, and V. Florea, "On the dynamics of population inversion for 3 μm Er^{3+} lasers," IEEE J. Quantum Electron. **29**(2), 426–434 (1993).
6. D. L. Sun, J. Q. Luo, Q. L. Zhang, J. Z. Xiao, W. P. Liu, S. F. Wang, H. H. Jiang, and S. T. Yin, "Growth and radiation resistant properties of 2.7–2.8 μm Yb,Er:GSGG laser crystal," J. Cryst. Growth **318**(1), 669–673 (2011).
7. G. Gross, A. L. Denisove, E. V. Zharikov, D. A. Zubenko, M. A. Noginov, U. Reimann, V. A. Smirnov, G. Huber, and I. A. Shcherbakov, "Depopulation of lower laser level $^4I_{13/2}$ Er^{3+} in YSGG:Cr:Er," Laser Phys. **1**(1), 52–56 (1991).
8. Y. Wang, Z. Y. You, J. F. Li, Z. J. Zhu, E. Ma, and C. Y. Tu, "Spectroscopic investigations of highly doped Er^{3+}:GGG and Er^{3+}/Pr^{3+}:GGG crystals," J. Phys. D Appl. Phys. **42**(21), 215406 (2009).
9. Y. Wang, Z. Y. You, J. F. Li, Z. J. Zhu, E. Ma, and C. Y. Tu, "Crystal growth and optical properties of Cr^{3+},Er^{3+}, RE^{3+}:$Gd_3Ga_5O_{12}$ (RE=Tm,Ho,Eu) for mid-IR laser applications," J. Lumin. **132**(3), 693–696 (2012).
10. J. Schneider, D. Hauschild, Ch. Frerichs, and L. Wetenkamp, "Highly efficient Er^{3+}:Pr^{3+}-codoped CW fluorozirconate fiber laser operating at 2.7 μm," Int J Infrared Milli. **15**(11), 1907–1922 (1994).
11. J. K. Chen, D. L. Sun, J. Q. Luo, J. Z. Xiao, H. X. Kang, H. L. Zhang, M. J. Cheng, Q. L. Zhang, and S. T. Yin, "Spectroscopic, diode-pumped laser properties and gamma irradiation effect on Yb, Er, Ho:GYSGG crystals," Opt. Lett. **38**(8), 1218–1220 (2013).
12. D. S. Knowles and H. P. Jenssen, "Unconversion versus Pr-deactivation for efficient 3 μm laser operation in Er," IEEE J. Quantum Electron. **28**(4), 1197–1208 (1992).

#194812 - $15.00 USD Received 29 Jul 2013; revised 11 Sep 2013; accepted 13 Sep 2013; published 25 Sep 2013

13. B. Y. Zhang, J. L. Xu, G. J. Wang, J. L. He, W. J. Wang, Q. L. Zhang, D. L. Sun, J. Q. Luo, and S. T. Yin, "Continuous-wave and passively Q-switched laser performance of a disordered Nd:GYSGG crystal," Opt. Commun. **284**(24), 5734–5737 (2011).
14. K. Zhong, J. Q. Yao, C. L. Sun, C. G. Zhang, Y. Y. Miao, R. Wang, D. G. Xu, F. Zhang, Q. L. Zhang, D. L. Sun, and S. T. Yin, "Efficient diode-end-pumped dual-wavelength Nd, Gd:YSGG laser," Opt. Lett. **36**(19), 3813–3815 (2011).
15. J. Y. Gao, Q. L. Zhang, D. L. Sun, J. Q. Luo, W. P. Liu, and S. T. Yin, "Energy levels fitting and crystal-field calculations of Nd^{3+} doped in GYSGG crystal," Opt. Commun. **285**(21-22), 4420–4426 (2012).
16. J. K. Chen, D. L. Sun, J. Q. Luo, J. Z. Xiao, R. Q. Dou, and Q. L. Zhang, "Er^{3+} doped GYSGG crystal as a new laser material resistant to ionizing radiation," Opt. Commun. **301–302**, 84–87 (2013).
17. J. S. Liu, J. J. Liu, and Y. Tang, "Performance of a diode end-pumped Cr,Er:YSGG laser at 2.79 μm," Laser Phys. **18**(10), 1124–1127 (2008).
18. I. Sokólska, E. Heumann, S. Kück, and T. Lukasiewicz, "Laser oscillation of Er^{3+}:YVO_4 and Er^{3+}, Yb^{3+}:YVO_4 crystals in the spectral range around 1.6 μm," Appl. Phys. B **71**(6), 893–896 (2000).
19. D. F. de Sousa, F. Batalioto, M. J. V. Bell, S. L. Oliveira, and L. A. O. Nunes, "Spectroscopy of $Nd^{3+}$and Yb^{3+} co-doped fluoroindogallate glasses," J. Appl. Phys. **90**(7), 3308–3313 (2001).
20. D. G. Lancaster and J. M. Dawes, "Thermal-lens measurement of a quasi steady-state repetitively flashlamp-pumped Cr,Tm,Ho:YAG laser," Opt. Laser Technol. **30**(2), 103–108 (1998).
21. B. J. Dinerman and P. F. Moulton, "3- μm cw laser operations in erbium-doped YSGG, GGG, and YAG," Opt. Lett. **19**(15), 1143–1145 (1994).
22. B. J. Dinerman, J. Harrison, and P. F. Moulton, Continuous wave and pulsed laser operation at 3 μm in Er^{3+}-doped crystals, in Advanced Solid-State Lasers, Vol. 24 of OSA Proceedings Series (Optical Society of America, Washington, D.C., 1994) pp. 168–170.

1. Introduction

Solid-state lasers at the wavelength region of 2.7–3 μm are useful for medical and biological applications because of the strong water absorption around this spectral region [1, 2]. In addition, 2.7–3 μm lasers are suitable pump sources for infrared optical parametric oscillation (OPO) or optical parametric generation [3, 4]. Er^{3+} serves as an active ion emitting 2.7–3 μm by $^4I_{11/2}\rightarrow{}^4I_{13/2}$ transition, which is commonly believed to be self-terminating because the lifetime of the upper laser level is less than that of the lower level. Highly doped concentrations (>30 at.%) of Er^{3+} ions are proposed to overcome this self-terminating "bottleneck" effect by inducing upconversion (UC_1) ($^4I_{13/2}\rightarrow{}^4I_{15/2}$) + ($^4I_{13/2}\rightarrow{}^4I_{9/2}\rightarrow{}^4I_{11/2}$) and cross-relaxation (CR) ($^4S_{3/2}$ ($^2H_{11/2}$) $\rightarrow{}^4I_{15/2}$) + ($^4I_{15/2}\rightarrow{}^4I_{13/2}$) + ($^4I_{15/2}\rightarrow{}^4I_{9/2}\rightarrow{}^4I_{11/2}$) processes [5] (Fig. 1). Both processes influence population inversion and produce an even population of the initial ($^4I_{11/2}$) and final ($^4I_{13/2}$) energy levels as a whole. Another upconversion process (UC_2) ($^4I_{11/2}\rightarrow{}^4I_{15/2}$) + ($^4I_{11/2}\rightarrow{}^4F_{7/2}\rightarrow{}^4S_{3/2}$) generates green and red emissions and deactivates the initial laser level, but this negative effect can be compensated for by the above mentioned CR process involving $^4S_{3/2}$ [5, 6]. Another method of reducing the lifetime of the lower laser level is the co-doping of deactivation ions [7–12], which is advantageous to population inversion. Pr^{3+} is a suitable ion because its energy level $^3F_4$ is adjacent to level $^4I_{13/2}$ of Er^{3+}. The energy transfer diagram between Er^{3+} and Pr^{3+} ions is shown in Fig. 1. AT denotes the pumping absorption transition, and ET_1 and ET_2 denote energy transfer from $^4I_{11/2}\rightarrow{}^1G_4$ and $^4I_{13/2}\rightarrow{}^3F_4$, respectively; the efficiencies of energy transfer are determined as 64.2% and 96.5% in Er,Pr:GGG crystal [8], respectively. Knowles and Jenssen have reported [12] in detail the Er:BaY_2F_8 crystal codoped with Pr ions can efficiently deactivate the terminal laser level and show several advantages, including allowing the laser to be operated at lower Er concentrations which reduces the losses associated with $^4I_{11/2}$ upconversion, and simplifying the dynamics by allowing quasi-4 level operation. Moreover, the new matrix GYSGG ($Gd_{1.17}Y_{1.83}Sc_2Ga_3O_{12}$) that is attracting considerable attention can be obtained by replacing some Gd^{3+} ions with Y^{3+} in GSGG ($Gd_3Sc_2Ga_3O_{12}$). This new matrix exhibits many advantages such as excellent dual-wavelength laser property in Nd:GYSGG crystal [13–15] and radiation resistance ability in Er:GYSGG crystal [11, 16].

In this work, we report for the first time the spectroscopic properties of Er,Pr:GYSGG crystals grown by the Czochralski method. A 968 nm diode end-pumped 2.79 μm laser operated in the CW and pulse modes is also demonstrated.

#194812 - $15.00 USD Received 29 Jul 2013; revised 11 Sep 2013; accepted 13 Sep 2013; published 25 Sep 2013

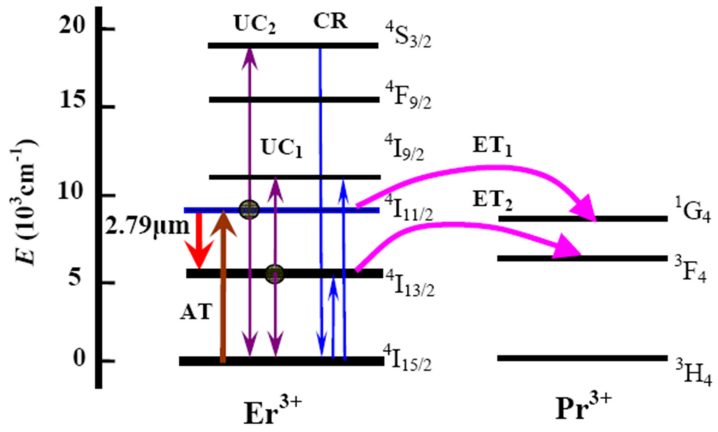

Fig. 1. Energy transfer diagram between Er^{3+} and Pr^{3+} ions.

2. Experimental details

An Er,Pr:GYSGG crystal was grown from a melt of congruent composition containing 20 at.% Er^{3+} and 0.3 at.% Pr^{3+} by the Czochralski method. The structural formula can be written as $(Er_{0.6}Pr_{0.009}Gd_{1.17}Y_{1.221})Sc_2Ga_3O_{12}$, which belongs to the space group of I_{a3d} with a cubic structure, and the lattice parameter is 12.4938 Å. Gd_2O_3, Ga_2O_3, and Sc_2O_3 powders (99.99% purity), as well as Er_2O_3 and Pr_2O_3 (99.999% purity), were used as starting raw materials and weighed according to the designed compositions. Ga_2O_3 was overweighed by 2 wt.% to compensate for evaporation loss during growth. Growth experiments were performed with the aid of an automatic diameter control unit operated in up-weighing mode. The pulling rate was 1 mm/h, and the seed rotation speed was 7 rpm. Er,Pr:GYSGG crystal with a high optical quality and dimensions of about Φ 25 mm × 100 mm was obtained. The photograph of the as-grown Er,Pr:GYSGG crystal is shown in Fig. 2. Sample disks were perpendicularly cut to the growth direction <111> from the post-annealing crystals and then polished on both sides. For spectral measurements, 2 mm-thick samples were used. For laser experiments, 2 mm × 2 mm × 5 mm samples were used. The absorption spectrum was recorded on a lambda 950 spectrophotometer (PerkinElmer, Inc, USA). A FLSP 920 fluorescence spectrometer (Edinburgh instrument Ltd, UK) was used to measure the fluorescence spectrum with a 968 nm laser diode (LD) excitation source, and fluorescence decay curves were obtained by excitation with an Opolette 355 I OPO laser (OPOTEK, Inc, USA).

Fig. 2. Photograph of as-grown Er,Pr:GYSGG laser crystal.

The configuration for generating laser output is shown in Fig. 3. The pump source was an InGaAs LD emitting up to 40 W at around 968 nm in CW mode, and it also can be operated in pulse mode controlled by the appropriate driving current waveform with the repetition rate of 1-1000 Hz and minimum pulse duration of 0.1 ms. The fiber-coupled pump laser was

#194812 - $15.00 USD Received 29 Jul 2013; revised 11 Sep 2013; accepted 13 Sep 2013; published 25 Sep 2013

collimated and focused onto an uncoated 2 mm × 2 mm × 5 mm Er,Pr:GYSGG crystal with parallel and polished end faces. The crystal was enclosed by a copper heat sink with cooling water passage. An indium film was placed between the Er,Pr:GYSGG crystal and copper heat sink for closer contact. A plane–plane cavity was used as a resonator, and the cavity lengths were 12, 15, and 18 mm, respectively. A K9 glass plate with antireflection coating of High transmission (HT) > 95% at 968 nm and reflectivity of 100% at 2.79 μm was used as the input mirror. The output mirrors (CaF_2 substrate) with different transmissions of 0.5%, 2%, and 5% at 2.79 μm were used to obtain the optimum laser output.

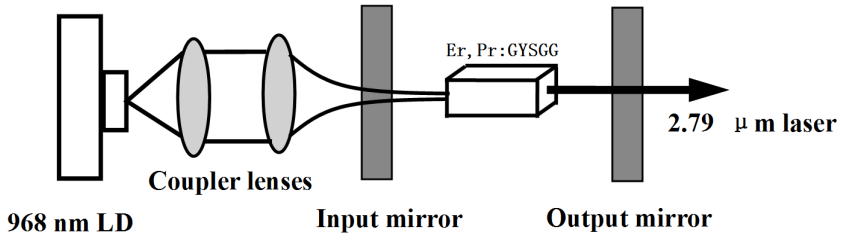

Fig. 3. Experimental setup of the Er,Pr:GYSGG laser.

3. Results and discussion

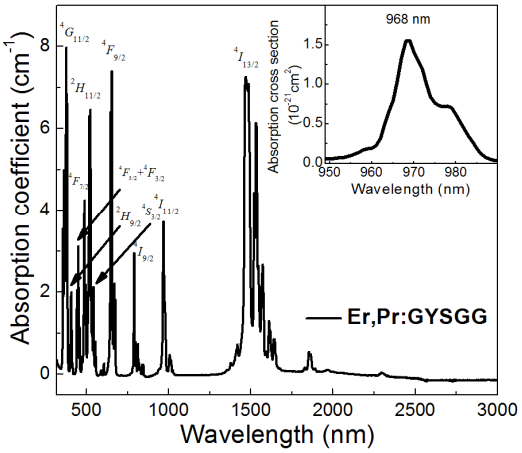

Fig. 4. Absorption spectrum of Er,Pr:GYSGG crystal. Inset: absorption cross section within the range of 950–990 nm.

The absorption spectrum of Er,Pr:GYSGG crystal is shown in Fig. 4. The main absorption bands are found to be centered at around 376, 407, 450, 486, 523, 544, 654, 790, 968, and 1478 nm, which correspond to the transitions from ground state $^4I_{15/2}$ to excited states $^4G_{11/2}$, $^2H_{9/2}$, $^4F_{5/2}$ + $^4F_{3/2}$, $^4F_{7/2}$, $^2H_{11/2}$, $^4S_{3/2}$, $^4F_{9/2}$, $^4I_{9/2}$, $^4I_{11/2}$, and $^4I_{13/2}$, respectively. The inset in Fig. 4 shows the absorption cross section within the wavelength range of 950-990 nm and the maximum absorption cross section at 968 nm is 1.6 × 10^{-21} cm^2. The full width at half-maximum of 968 nm absorption band is about 15 nm, which is relatively suitable and desirable for efficient pumping by high-power InGaAs laser diodes. The Er^{3+} ions can be

#194812 - $15.00 USD Received 29 Jul 2013; revised 11 Sep 2013; accepted 13 Sep 2013; published 25 Sep 2013

directly pumped into upper laser level $^4I_{11/2}$ by radiation at around 970 nm and can avoid various non-radiative losses and thermal loading [17].

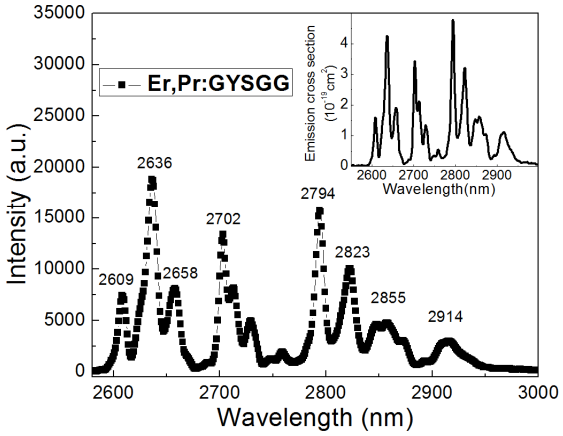

Fig. 5. Fluorescence spectrum of Er,Pr:GYSGG crystal excited by a 968 nm LD. Inset: emission cross section curve.

The fluorescence spectrum of Er,Pr:GYSGG crystal excited by a 968 nm LD is shown in Fig. 5. Many fluorescence peaks (2609, 2636, 2658, 2702, 2794, and 2823 nm) are observed within 2.6–3 μm, and these peaks result from the transitions of stark sub-levels from $^4I_{11/2}$ to $^4I_{13/2}$. In addition, we calculate the stimulated emission cross-section based on the Füchtbauer–Ladenburg equation [18]

$$\sigma_{em}(\lambda) = \frac{\lambda^5 \cdot I(\lambda)}{8\pi n^2 c \tau_m \int \lambda I(\lambda) d\lambda} \tag{1}$$

where $I(\lambda)$ is the fluorescence intensity, τ_m is the measured lifetime of the upper energy level, c is the velocity of light, n is the refractive index, and λ is the emission wavelength. The maximum emission cross section value at 2.79 μm is as high as 4.7×10^{-19} cm^2, as shown in the inset of Fig. 5, which is beneficial for obtaining low-threshold and high-efficiency laser output.

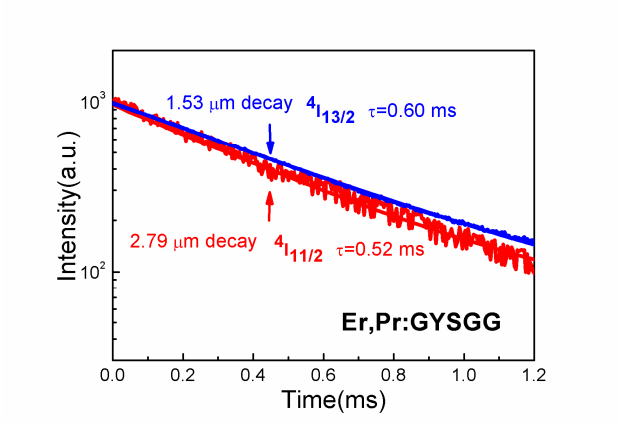

Fig. 6. Fluorescence decay curves of Er,Pr:GYSGG crystal.

#194812 - $15.00 USD Received 29 Jul 2013; revised 11 Sep 2013; accepted 13 Sep 2013; published 25 Sep 2013

The fluorescence decay curves of 2.79 and 1.53 μm excited by OPO show single exponential decay behavior, corresponding to the lifetimes of upper level $^4I_{11/2}$ and lower level $^4I_{13/2}$ at 0.52 and 0.60 ms, respectively (Fig. 6). By contrast, the lifetime of upper level $^4I_{11/2}$ is 1.2 ms and that of the lower level $^4I_{13/2}$ is 3.9 ms in Er:GYSGG [16]. This finding indicates that Pr^{3+} can depopulate the Er^{3+}:$^4I_{11/2}$ and $^4I_{13/2}$ levels by resonant energy transfer to Pr^{3+}: $^1G_4$ (ET_1) and $^3F_4$ (ET_2) (Fig. 1), respectively. In addition, the energy transfer efficiency of Er→Pr can be calculated from [19]

$$\eta_\tau = 1 - \frac{\tau_1}{\tau_2} \tag{2}$$

where τ_1 is the lifetime of Er:GYSGG and τ_2 is the lifetime of Er,Pr:GYSGG. Based on Eq. (2) and the aforementioned lifetime values of Er:GYSGG and Er,Pr:GYSGG, the energy transfer efficiencies of Er→Pr in ET_1 and ET_2 are 56.7% and 84.6%, respectively. Therefore, the energy transfer rate of ET_2 is greater than that of ET_1, which is advantageous to the improvement of 2.7–3 μm laser performance. As the efficiency of energy transfer from Er to Pr strongly relies on the concentration of both dopants [12], a suitable concentration ratio between Er and Pr could keep the $^4I_{11/2}$ as long as possible while significantly reduce the $^4I_{13/2}$ lifetime.

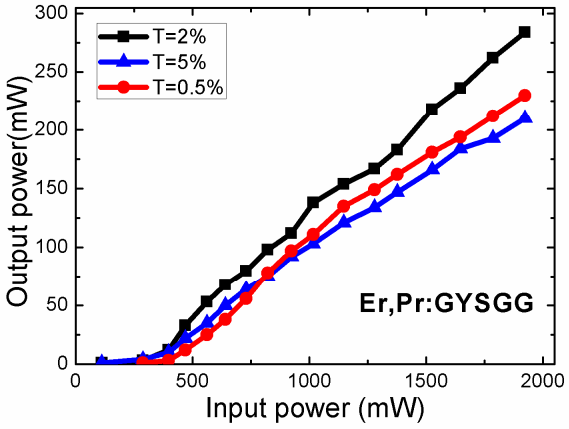

Fig. 7. Dependence of laser output energy with different transmissions of the output coupler in the CW mode.

Figure 7 shows the laser output power as a function of input pump power for different transmissions of output coupling mirror. The pump laser is operated in the CW mode, and the cavity length is maintained at 12 mm. The output coupler with a transmission of 2% generates the better results than the others. The maximum laser power of 284 mW corresponding to the threshold of 112 mW is obtained. Linear fitting results show 14.8% optical-to-optical efficiency and 17.4% slope efficiency. At 150 mW output power, the far-field divergence of 6.2 mrad and M^2 factor of 1.72 were determined using the knife-edge method. This value of slope efficiency (17.4%) of Er,Pr:GYSGG is larger in compared with that of Er:GYSGG (10.1%). The laser threshold is also lower than that of Er:GYSGG, which can be attributed to the doping of deactivator Pr^{3+} ions that can reduce the lower-level lifetimes of Er^{3+} by resonant energy transferring. Meanwhile, the maximum laser output power 284 mW is lower than the reported value (348 mW) for Er:GYSGG [16], which may be due to the fact that the shortened lifetime of upper level $^4I_{11/2}$ is detrimental to energy storage during diode CW pumping.

#194812 - $15.00 USD Received 29 Jul 2013; revised 11 Sep 2013; accepted 13 Sep 2013; published 25 Sep 2013

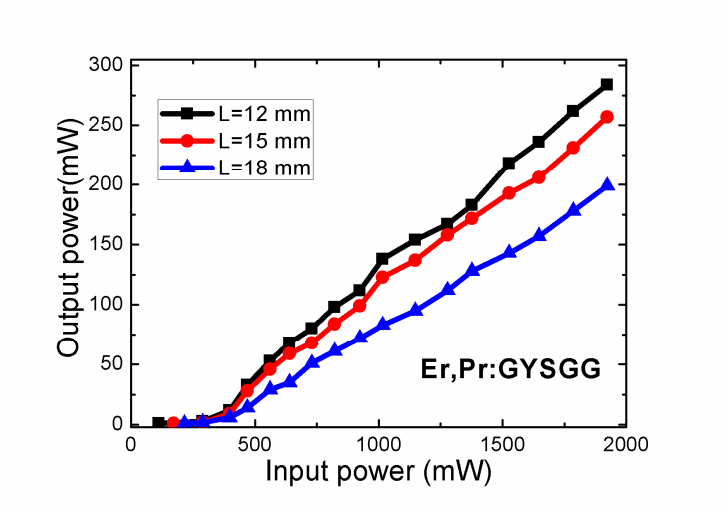

Fig. 8. Laser output power versus input power for different cavity lengths.

The influence of cavity length on laser output power at 2% transmission of the output coupler was investigated, and the results are shown in Fig. 8. Notably, the laser output power decreases with increasing cavity length. This phenomenon is mainly due to the thermal lens effect in Er,Pr:GYSGG crystal, resulting in larger diffraction losses in a longer cavity [17, 20]. Therefore, a shorter cavity and a better cooling setup can improve the laser output power and efficiency. Dinerman et al. [21] reported a CW mode pumped Er:YSGG crystal with 511 mW output power and slope efficiency up to 26% using two end surfaces of the crystal as resonant cavity. In the future, we will optimize crystal size and cavity structure to improve the laser performance of Er,Pr:GYSGG.

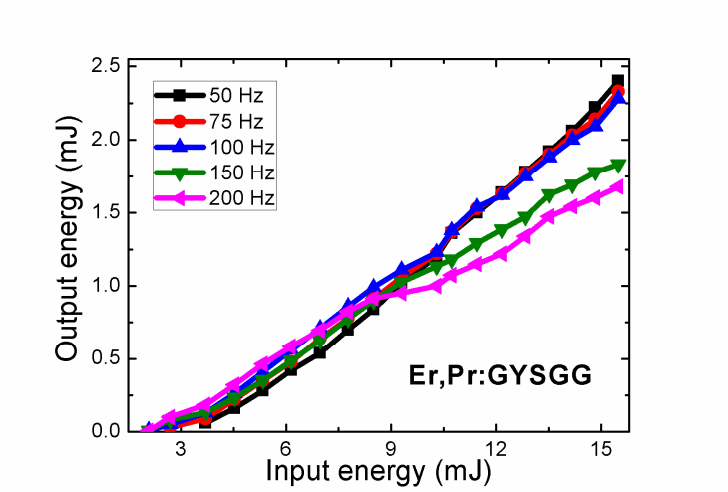

Fig. 9. Laser output energy versus input energy at different repetition rates.

The laser output energy versus the pump energy at different repetition rates of 50, 75, 100,150 and 200 Hz are shown in Fig. 9. Meanwhile, an output coupler with 2% transmission, pulse duration with 0.5 ms and 12 mm-long cavity was used throughout the entire experiment. The laser output energy exhibits moderate difference below the repetition rate of 100 Hz. In addition, it can be seen that at low pump energy the slope efficiency is much higher and falls after a certain roll-over point with increasing energy when the repetition rate is >100 Hz. The

#194812 - $15.00 USD Received 29 Jul 2013; revised 11 Sep 2013; accepted 13 Sep 2013; published 25 Sep 2013

phenomenon can be attributed to the fact that a plane-plane resonator is very sensitive against thermal lensing, leading to the slope efficiency measurements distorted dramatically at a higher repetition rate and larger pumping energy. The plane-concave or V-type resonators are more stable and could allow the crystal to be operated at a higher repetition rate. The maximum output energy of 2.4 mJ corresponding to the peak power of 4.8 W is obtained when the repetition rate is 50 Hz. Linear fitting results show optical-to-optical efficiency of 15.5% and slope efficiency of 18.3%. Under similar laser configurations, Liu et al. [17] reported a maximum peak power of 970 mW with a pulse duration 2 ms and slope efficiency of 7.6% in Cr,Er:YSGG. Dinerman et al. [22] obtained a peak power of 3.4 W with a pulse duration of 1 ms and slope efficiency of 9.1% on a quasi-CW diode end-pumped Er:YSGG.

The increasing laser efficiency and decreasing laser threshold of Er,Pr:GYSGG crystal are due to the doping of deactivator Pr^{3+} ions. However, the maximum laser output power and the performance operating at high repetition rate are only close to those of the Er:GYSGG [16]. Therefore, further studies may focus on optimizing the concentration ratio of Pr^{3+} to Er^{3+} and cavity parameters to improve the laser performance of Er,Pr:GYSGG crystal entirely.

4. Conclusions

We report for the first time the spectroscopic and diode end-pumped laser properties of Er,Pr:GYSGG crystal grown by the Czochralski method. The lifetimes for the upper laser level $^4I_{11/2}$ and lower level $^4I_{13/2}$ are 0.52 and 0.60 ms, respectively, which are due to the doping of Pr^{3+} ions. The laser produces 284 mW of power in the CW mode, corresponding to a slope efficiency of 17.4%. The minimum laser threshold is only 112 mW. The maximum laser energy achieved is 2.4 mJ at a repetition rate of 50 Hz and pulse duration of 0.5 ms, corresponding to a peak power of 4.8 W and a slope efficiency of 18.3%. These results suggest that doping deactivator Pr^{3+} ions can decrease lower-level lifetime and effectively improve laser efficiency.

Acknowledgments

This work was financially supported by the National Natural Science Foundation of China (Grant Nos. 91122021, 51272254, 61205173, 51172236, and 50932005).

#194812 - $15.00 USD Received 29 Jul 2013; revised 11 Sep 2013; accepted 13 Sep 2013; published 25 Sep 2013